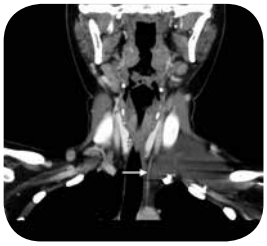

Lesions of the Thoracic Operculum on CT and MRI: Between the Neck and the Chest

Lesiones del opérculo torácico en TC y RM: Entre el cuello y el tórax

Felipe Aluja Jaramillo[1]
Juan Andrés Mora Salazar[2]

Key words (MeSH)
Vascular system injuries
Tomography, X-ray
Magnetic eesonance imaging

Summary

The thoracic inlet is located in the anatomic boundaries between the neck and the thorax. There is a wide variety of entities that can be found in this area including lesions of vascular origin, pathology involving the digestive tract and airways, as well as entities affecting the lymphatics and neural structures. Benign and malignant tumors of the thorax and neck can spread through the thoracic inlet, with goiter and lymphoproliferative neoplasms being the most common. It is important for the radiologist to know the anatomy and pathology that can be found in the thoracic inlet as, given its location, it can often been unnoticed.

Palabras clave (DeCS)
Lesiones del sistema vascular
Tomografía por rayos X
Imagen por resonancia magnética

Resumen

El opérculo torácico se encuentra localizado entre los límites anatómicos del cuello y el tórax. En esta área se puede encontrar diversidad de patologías, entre ellas, de tipo vascular, del tracto digestivo y la vía aérea, de origen linfático y neural. Las lesiones tumorales de tipo benigno o maligno, que se originan en el cuello o en el tórax, pueden diseminarse a través del opérculo; las más comunes son el bocio de origen tiroideo y las neoplasias de origen linfoproliferativo. Es importante que el radiólogo conozca la anatomía y las patologías que se pueden encontrar en el opérculo torácico, pues, por su localización, muchas veces pasan inadvertidas.

Introduction

El opérculo torácico (OT) es un área de transiciónThe thoracic operculum (TO) is a transition area between the neck and thorax that usually involves the last image acquired in a neck study and the first image acquired in a chest study, therefore, is part of the region of interest of neck and chest radiologists. The anatomy in this area is complex due to its multiple anatomical structures, so that some injuries can go unnoticed (1,2).

Some lesions that originate in the neck or thorax can cross through the TO in an ascending or descending direction, others, on the contrary, are located and remain in this location.

The objective of this study is to characterize the relevant anatomy in TO images, describe the most frequent lesions in this location according to their origin ascending or descending through the TO and describe the relevant imaging findings in each of these entities.

Anatomy of the thoracic operculum

The TO is an anatomical region that is characterized by its symmetry on both sides of the midline (1), and directly communicates the neck and thorax (3). It is delineated by Sibson's fascia extending from the transverse processes of C7 to the medial edge of the first rib (3,4). The TO lies in an oblique plane, is higher in the posterior part and longer in its transverse diameter than in the anteroposterior diameter (3,4). It is surrounded by bony structures: the body of the first rib is its posterior and superior border, the first two ribs and rib cartilages form the lateral and anterior borders, and the anterior and inferior border forms it in the sternum (2,3). The pulmonary apices are located in the posterior aspect of the operculum due to its oblique orientation and the key structures that pass through it are located more anterior (figure 1) (2,3).

The fascias of the infrahyoid neck extend through the TO to the mediastinum dividing it into

[1]Radiologist, Country Scan Ltd. Bogotá, Colombia.

[2]Radiologist, Clinica Universitaria Colombia. Bogotá, Colombia.

different compartments or spaces each with their respective contents (figure 1) (2).

Its main content is broken down in table 1.

Table 1. Normal contents of the thoracic operculum

Vascular structures	Neural structures
Brachycephalic trunk Common carotid artery left Left subclavian artery Internal jugular veins Subclavian veins	Vagus nerve Recurrent laryngeal nerve Phrenic nerve Cervical sympathetic plexus Brachial plexus
Lymphatic structures	**Structures of the gastrointestinal tract**
Lymph nodes Thoracic duct	Proximal esophagus
Airway structures	**Bony structures**
Windpipe Pulmonary apices	Vertebral bodies (C7 to T2) Three first costal arches Handle of the sternum

From the knowledge of this anatomy, you can break down the entities that are in this anatomical region. The differential diagnosis of TO lesions is varied and the different possible origins of a lesion must be taken into account for an adequate imaging approach.

Vascular lesions

Aberrant right subclavian artery

The left aortic arch associated with an aberrant right subclavian artery is the most common congenital anomaly of the aortic arch (5). It occurs between 0.5 and 2% of the population (5,6). It is the result of a regression of the right arcus and right ductus arterious with persistence of the right dorsal aorta in its distal portion, which will then be the aberrant right subclavian artery (5).

In most cases, patients are asymptomatic; in symptomatic cases, patients manifest dysphagia secondary to compression of the esophagus by the artery (called lusory dysphagia) (5,7). It is associated with the right recurrent laryngeal nerve with a "non-recurrent" course.

Anatomically, the aberrant right subclavian artery originates directly from the aortic arch, as the last branch, with an oblique and posterior path to the esophagus (5). Due to this, the main finding in images is of a vascular structure, which enhances in the arterial phase, located in the retroesophageal area (figure 2).

Characteristically, this entity can be associated with other thoracic vascular malformations, including: aortic coarctation, patent ductus arteriosus, and interventricular communication (5,8).

Dissections, thrombosis and arterial aneurysms

Arterial thrombosis is a rare entity secondary to severe atherosclerotic disease (9). It occurs most frequently in the carotid arteries, even with thrombi floating within these arteries (10). The symptoms are variable depending on the degree of obstruction and the most frequent clinical presentation in the occlusion of the common carotid artery is the cerebrovascular event (figure 3).

The dissection refers to the accumulation of blood between the layers of the wall of the artery (11). It is usually secondary to trauma or non-traumatic causes (atherosclerotic or spontaneous disease) (11). Other less frequent etiologies, such as fibromuscular dysplasia, Behçet's disease and even Takayasu's arteritis can be causes of dissection in the carotid arteries (12). Traumatic dissection is usually located in the common carotid artery, tends to result in complete occlusion and does not resolve on its own (11). It is often more common for these dissections to be presented distal to the TO (figure 4).

Venous thrombosis

The most frequently compromised vein is the internal jugular vein. The causes of thrombosis are varied, the most frequent being secondary to central catheter. Other causes are local infection, compression by mediastinal masses or neoplasms (Trousseau's syndrome); Trauma and intravenous drug use are less frequent but not rare (13,14). In postoperative cases it has been described that up to 1/3 of patients can develop internal jugular vein thrombosis (14).

Clinically, it is characterized by edema and pain on the affected side, sensation of mass and fever (13). Among the most frequent complications is embolism, usually septic, to the central nervous system (13). When the thrombus is infected by extension of an oropharyngeal infection it is called Lemierre's syndrome (14).

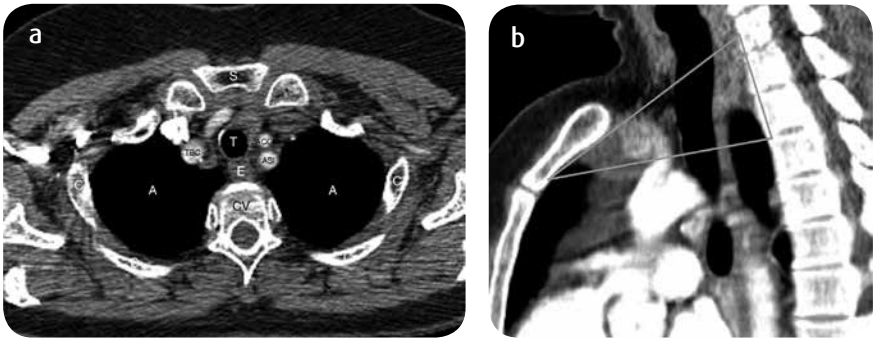

Figure 1. a) CT axial slice and b) sagittal reconstruction. Normal anatomy of the thoracic operculum marking each of the main structures and the limits in the sagittal reconstruction (lines). A: pulmonary apices, CV: vertebral body, E: esophagus, T: trachea, TBC: brachiocephalic trunk, ACCI: left common carotid artery, ASI: left subclavian artery, S: sternum, C: costal arches.

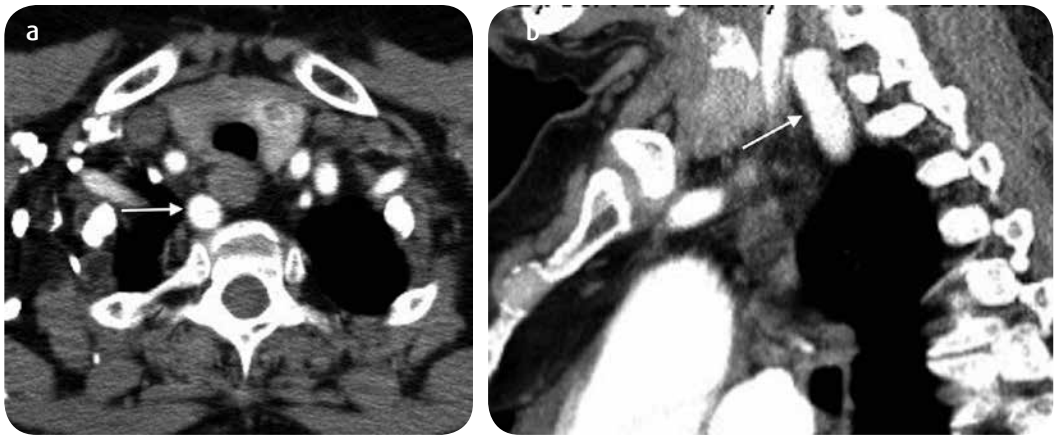

Figure 2. a) CT axial cut and b) sagittal reconstruction. A retroesophageal (aberrant) course of the right subclavian artery is observed (arrow).

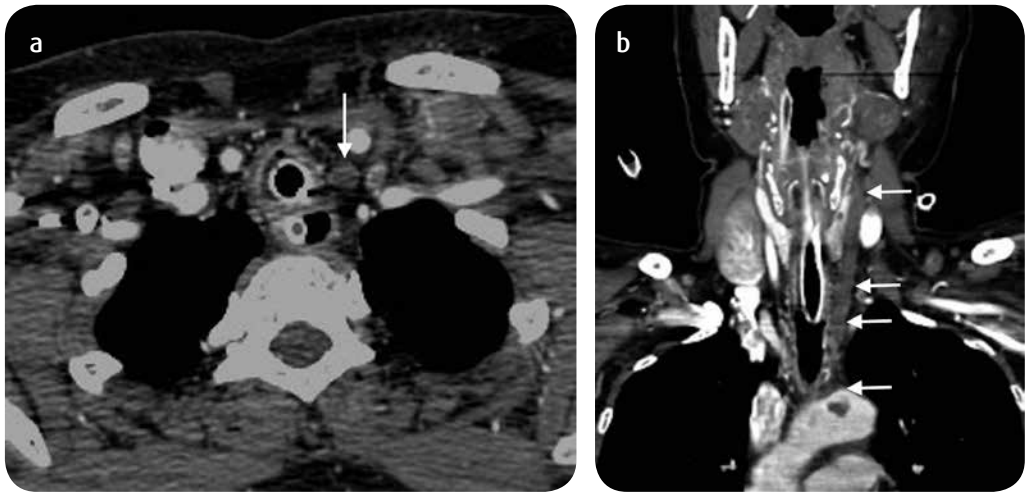

Figure 3. a) CT axial slice and b) coronal reconstruction. There is an absence of contrast medium and hypodense material in the lumen of the left common carotid artery, which originates from the aortic arch (arrows), findings related to arterial thrombosis.

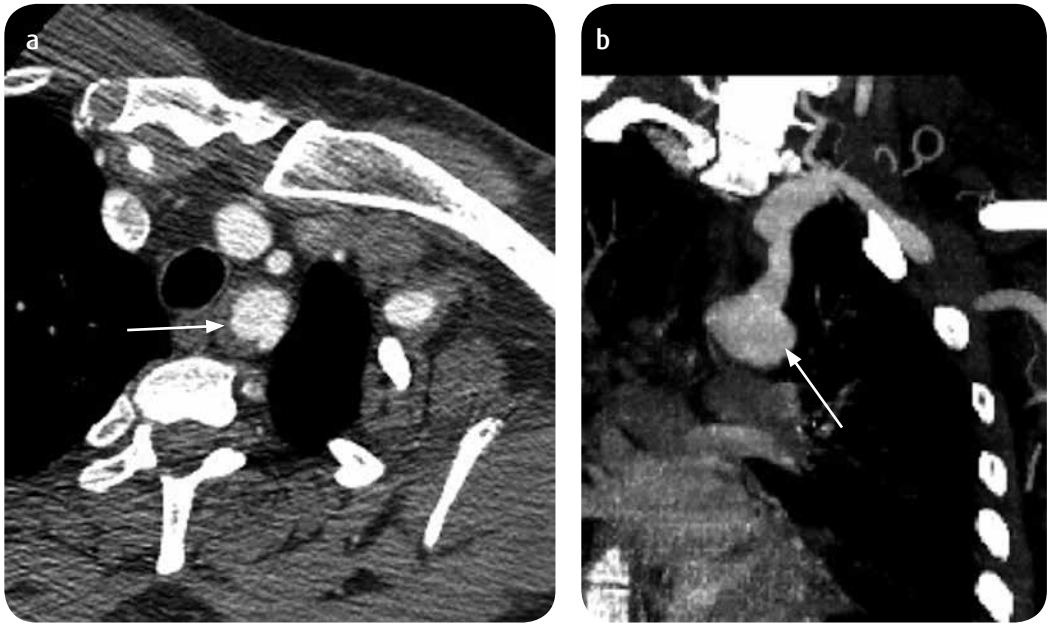

Figure 4. a) CT axial slice and b) coronal reconstruction. Dilation of the proximal segment of the left subclavian artery (arrows) with posteromedial mural thrombus related to aneurysm.

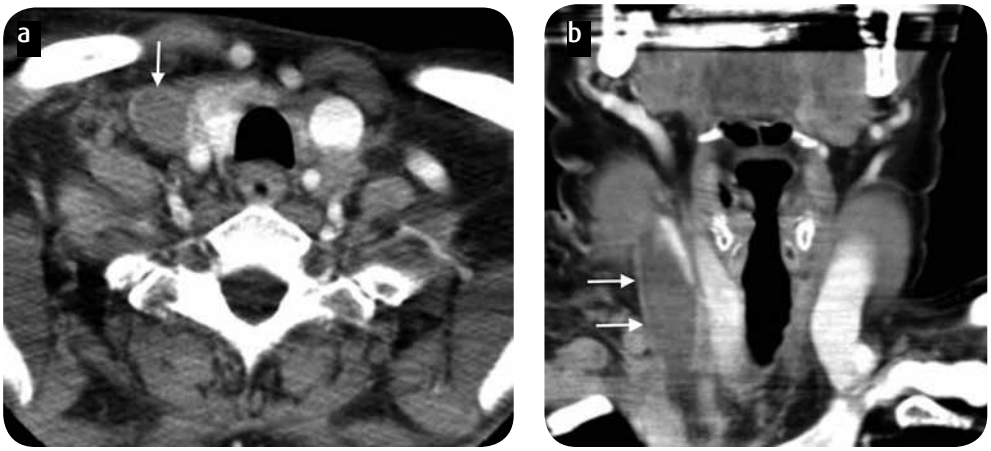

Figure 5. a) CT axial slice and b) coronal reconstruction. Low density material is seen inside the right internal jugular vein, with discrete peripheral enhancement related to venous thrombosis (arrows).

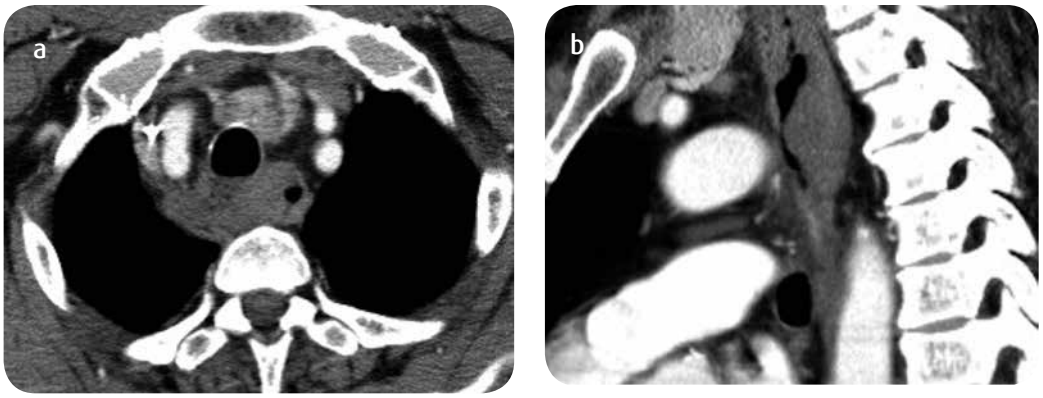

Figure 6. a) CT axial slice and b) sagittal reconstruction. Thickening of the esophageal wall with medium density material in the thickness of the wall (arrows) that generates a decrease in the amplitude of the esophageal lumen. Findings related to esophageal dissection and associated esophageal hematoma.

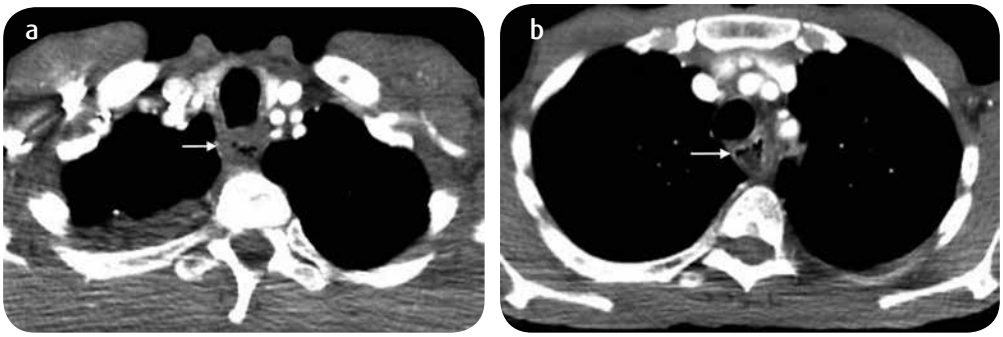

Figure 7. a and b) CT axial slice. Concentric thickening of the walls of the proximal esophagus related to esophageal carcinoma (arrows).

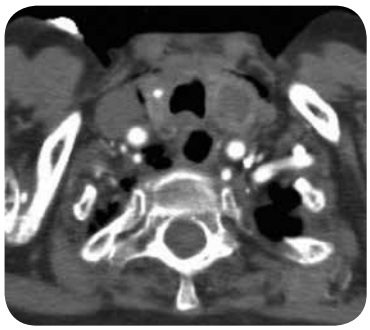

Figure 8. CT axial slice. Air is seen in the soft tissues of the neck that dissects the cervical fascias with extension to the mediastinum through the TO. There is striation and alteration of adjacent fat due to inflammatory changes compatible with a retropharyngeal abscess and descending mediastinitis.

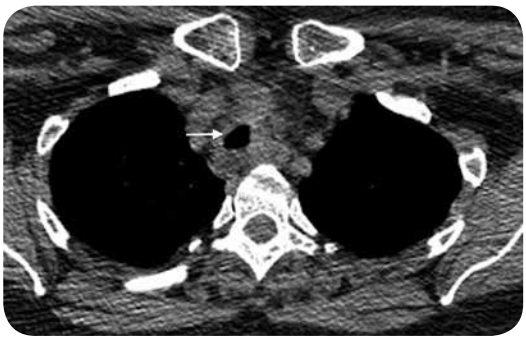

Figure 9. CT axial slice. Patient with tracheal stenosis after prolonged intubation (arrow).

The diagnosis in computed tomography (CT) is made when an increase in the diameter of the vein is found, with low density material inside the vessel and peripheral enhancement due to the passage of contrast medium through the vasa vasorum in the venous walls (figure 5) (13)

Esophageal lesions

Esophageal dissection

It is a rare entity also known as intramural hematoma or intramural rupture (15). Most often, it appears as a consequence of recent instrumentation; however, it can be associated with foreign bodies or Mallory-Weiss syndrome (15). Spontaneous esophageal hematomas have been reported in patients who are anticoagulated or have coagulopathies (15-17). The most frequent symptoms are retrosternal thoracic pain, dysphagia and odynophagia, and haematemesis, which is later and less frequent (15,17).

In CT with gas or contrast medium, a dissection line of the submucosa can be seen, with a double lumen appearance (figure 6) (15). The extension of this dissection is better evidenced in coronal or sagittal images (15); it usually occurs in the back of the true lumen of the esophagus.

The esophageal dissection is managed conservatively, with resolution in days or weeks (15-17).

Esophageal carcinoma

The proximal third of the esophagus is the least affected by esophageal cancer. It is usually of the squamous cell carcinoma type, and the main risk factors are smoking and alcoholism (18). It is more common in men (65%) with ages between 60 and 74 years old (18).

The symptoms described by patients suffering from this entity are dysphagia (progressive), odynophagia and weight loss (18).

CT usually involves thickening of the esophageal wall, initially asymmetric and later concentric, which is enhanced after administration of the contrast medium, especially in the arterial phase, rarely with associated soft tissue mass (figure 7) (18). Mediastinal invasion is suspected when there is alteration of the mediastinal fat, displacement or irregularity of the trachea or other mediastinal structures (18). Additionally, enlarged lymph nodes adjacent to the esophagus help establish the diagnosis of esophageal carcinoma (18,19).

Injuries of retropharyngeal and trachea

Retropharyngeal abscess and descending mediastinitis

Retropharyngeal abscess is secondary to a polymicrobial infection that originates in the oropharynx or cervical spaces, is characterized by its extension from the neck to the mediastinum through the TO, where it can produce descending mediastinitis.

There are three routes for the spread of these infections: 1) pretracheal, ends in the anterior mediastinum; 2) lateral pharyngeal, ends in the middle mediastinum; and 3) retropharyngeal, ends in the posterior mediastinum (20). It is recommended to perform CT studies with contrast medium in patients with cervical infections that include the upper portion of the thorax, to determine the extent of the infection (20).

The CT findings are thickening of the cervical tissues, including the cervical fascia and the muscles, areas of heterogeneous enhancement after the administration of the contrast medium, liquid collections that enhance the periphery after the administration of the contrast medium and adenomegalies of the reactive aspect (20). In some cases subcutaneous emphysema, edema and emphysema of the prevertebral soft tissues and, less frequently, septic vein thrombosis can be found (20). Mediastinal alteration of the mediastinal fat, fluid mediastinal collections with or without gas and sometimes pericardial effusion are usually found in the mediastinum (figure 8) (20).

Tracheal stenosis

La estenosis traqueal es usualmente secundaria a intubación prolonTracheal stenosis is usually secondary to prolonged intubation (either endotracheal tube or tracheostomy cannula), but it can also be postinfectious (tuberculosis), post-transplant or secondary to systemic diseases (amyloidosis, sarcoidosis, granulomatosis with polyangiitis, among others) (twenty-one).

Stenosis occurs as a result of necrosis of the tracheal wall due to high pressures over prolonged times (21). The prevalence varies between 1% and 20%, and is higher when high pressure cuffs are used (21). In patients with endobronchial tuberculosis, up to 90% of them develop postinfectious stenosis and in post-transplant patients up to 50% (21).

In CT the stenosis appears as an area of diminution of caliber of the trachea, usually extended in an approximate length of 2 cm and an "hourglass" morphology (figure 9) (21). Eccentric tracheal stenosis is less frequent (21).

Postinfectious stenoses tend to be longer and look like an asymmetric or focal thickening of the tracheal wall (21). Likewise, it may be secondary to extrinsic compression due to mediastinal lymph nodes or thyroid masses (21,22).

Post-transplant stenosis usually occurs at the site of the anastomosis and in addition to the decrease in caliber, signs of dehiscence of the anastomosis can be found (21).

Management with stenting or surgical resection and reconstruction may be indicated in more severe cases and, depending on the etiology, balloon dilation may be a therapeutic option (21).

Tracheal diverticulum

Tracheal diverticula are invaginations of the tracheal wall (23). They can be single or multiple and are classified as congenital or acquired (23). The congenital tracheal diverticulum represents a vestige of a supernumerary lung or a high division of the primary pulmonary outbreak (23,24). It is more frequent in men, appears 4 to 5 cm below the vocal cords with a small communication with the light of the trachea (23,25). It has the same histological characteristics of the trachea and usually contains mucus in its interior (23,26). The acquired tracheal diverticulum can appear anywhere in the trachea, more usual in the intrathoracic trachea, in the TO, tend to be larger and with a communication with the upper tracheal lumen (23). They

result from an increase in the intraluminal pressure of the trachea with a secondary herniation of the mucosa through the tracheal wall (23), and it is more frequent in patients with chronic respiratory symptoms or chronic cough (23,24,27). The characteristic of the Mounier-Khun syndrome are the multiple tracheal diverticula (23,26,28). Patients may be asymptomatic or manifest chronic or recurrent infections (23,29).

CT is the best imaging method for diagnosis, given its characteristics and the possibility of identifying communication with the trachea. They are thin-walled lesions, which contain air inside, are located in the posterolateral paratracheal region, most often to the right of the midline, usually not exceeding 3 cm in greatest diameter (figure 10) (23,30) .

Within the differential diagnoses to be considered are laryngocele, pharyngocele, Zenker's diverticulum, apical pulmonary hernias and pulmonary bullae (23,25).

Injuries of the lymphatic system

Lymphangioma

It is a benign congenital lesion of the lymphatic system, secondary to the excessive proliferation of lymphatic vessels (31). These tumors have the characteristic of invading or surrounding normal structures (4). Approximately 75% of lymphangiomas occur in the neck, posterior to the sternocleidomastoid muscle, and between 3 and 10% extend to the mediastinum (4,32), in some cases through TO. In the mediastinum, this type of lesion corresponds between 0.7% and 4.5% of the mediastinal masses (33).

CT and MRI are multilobulated, cystic appearance masses, with septa in the interior, which enhance in a variable manner, especially in the septa (more frequent when there is infection or surgical history) (figure 11) (4,32). Some lesions may have higher density or intensity of blood signal in MRI, as well as liquid-liquid levels in the interior (4).

Thoracic duct injuries

The thoracic duct is the trunk of the body's largest lymphatic drainage (34,35). It originates in the cisterna of the chyle at the height of L1, passes through the anterior margin of the thoracic spine, passes anteriorly and to the left in the TO and inserts in the innominate vein, in the internal jugular vein or in the left subclavian vein (35,36).

Thoracic duct injuries usually end in the formation of chylothorax (figure 12) (31). Most of them are of traumatic origin, occur in approximately 2% of cases of trauma, in conjunction with other lesions of the thorax, and in less than 0.1% of cases are isolated lesions (31). Visualizing the lesion is complex, due to the size of the duct, but it can be assumed when there is pleural effusion of lower density to the serous fluid and along the path of the lesion (31). The use of CT is used to document the presence and persistence of chylothorax (31).

Neural lesions

Brachial plexus injuries

The most frequent lesion of the brachial plexus is secondary to trauma (37). The vast majority of patients with these injuries have been involved in traffic accidents (37,38). A smaller proportion of lesions are seen in neonatal or young patients secondary to other etiologies (Erb's palsy or Duchenne's palsy) (37,38). The symptoms depend on the branches of the brachial plexus involved. In traffic accidents, branches from C7 to T1 are usually involved, triggering symptoms related to Horner's syndrome (37,38). Lesions can be classified as preganglionic, postganglionic or a combination of both (38). Preganglionic lesions affect the origin of nerve roots while postganglionic lesions affect the distal structure of the nerve (38).

Imaging of the brachial plexus should be done using MRI. The findings that can be identified are pseudomeningoceles, absence or discontinuity of the branches of the brachial plexus, lateral displacement of the branches of the brachial plexus, hemorrhage and inflammatory changes (figure 13) (37,38).

Schwannoma and neurofibroma

Schwannomas and neurofibromas are the most common benign tumors of the neural sheaths (1,39). They may appear as solitary lesions, although in patients with neurofibromatosis they are usually multiple (1). Both etiologies, despite having a different histology, have a similar imaging appearance (1).

Schwannomas usually involve the sympathetic plexus; however, they can affect the branches of the cervical nerves and the lower cranial nerves (1). They are well-circumscribed lesions, with soft tissue signal density and intensity, which present posterior enhancement to the medium of the contrast medium (figure 14) (1).

Neurofibromas are well-circumscribed, heterogeneous masses, usually of low signal intensity in T1-weighted sequences, high signal intensity in T2-weighted sequences and heterogeneous enhancement after administration of the contrast medium (figure 15) (4).

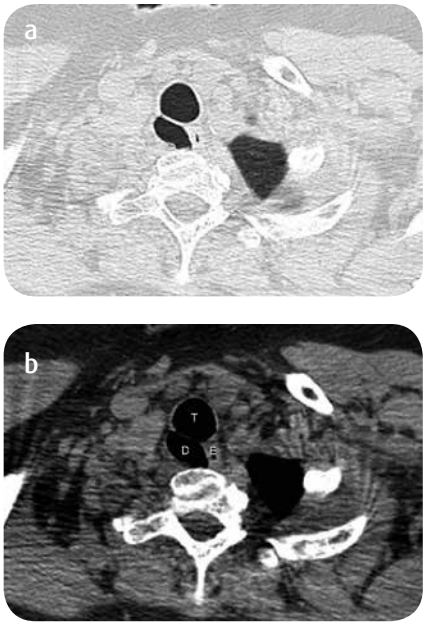

Figure 10. a and b) CT axial slice. Oval image with air inside, located in the posterolateral aspect of the trachea (T) with apparent communication with it (not shown) and in close relation with the esophagus (E). This finding corresponds to a tracheal diverticulum (D).

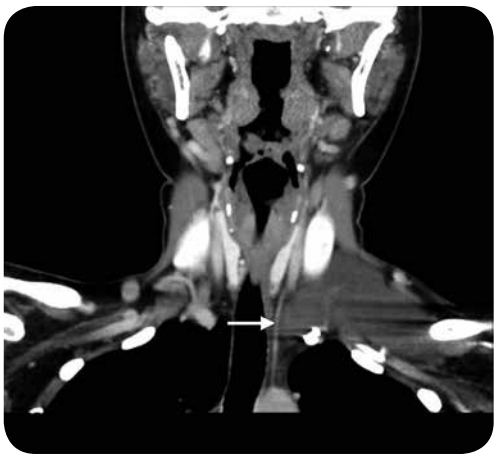

Figure 11. CT with coronal reconstruction. Oval lesion, predominantly hypodense, with some small septa inside, which does not enhance after the contrast medium; located in the left supraclavicular region and extended to the superior mediastinum through the TO (arrow). Corresponds to lymphangioma.

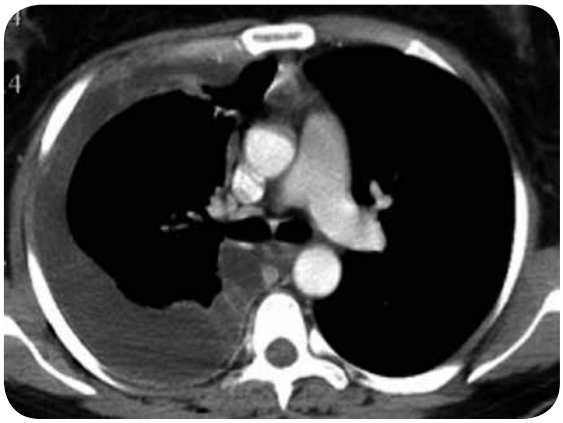

Figure 12. CT axial slice. Patient with a history of closed chest trauma. There is a right pleural effusion with low density (-5UH) suggestive of chylothorax.

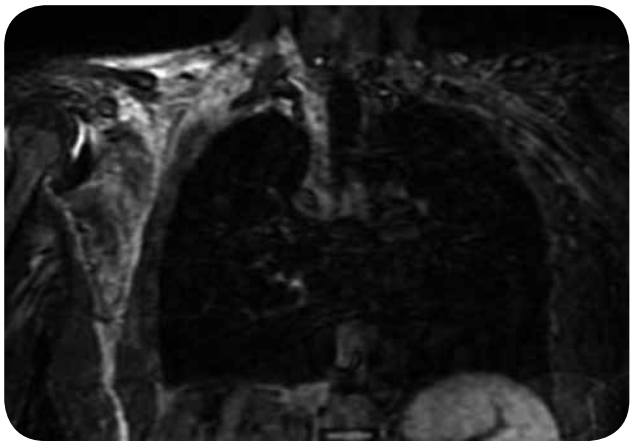

Figure 13. MRI, STIR axial sequence. High signal area in the right supraclavicular region and around the brachial plexus is appreciated due to changes in edema in a patient with a recent traumatic history, with damage to the brachial plexus nerves.

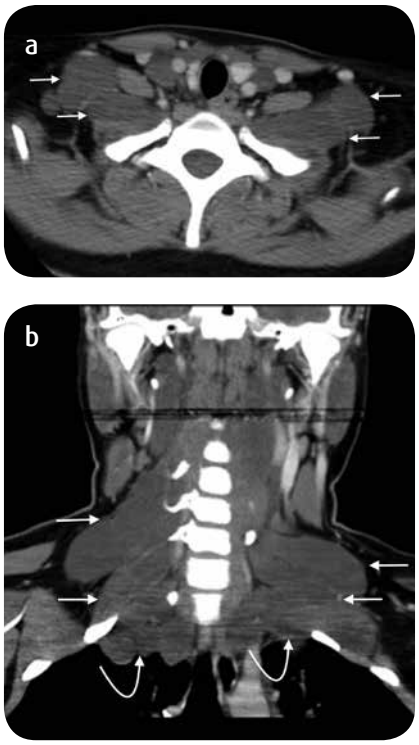

Figure 14. a) CT axial slice and b) coronal reconstruction. Predominantly, low density and homogeneous masses are observed, which extend from the conjunct holes of the cervical vertebral bodies (straight arrows) and through the TO (curved arrows), all of them related to schwannomas in a patient with schwannomatosis.

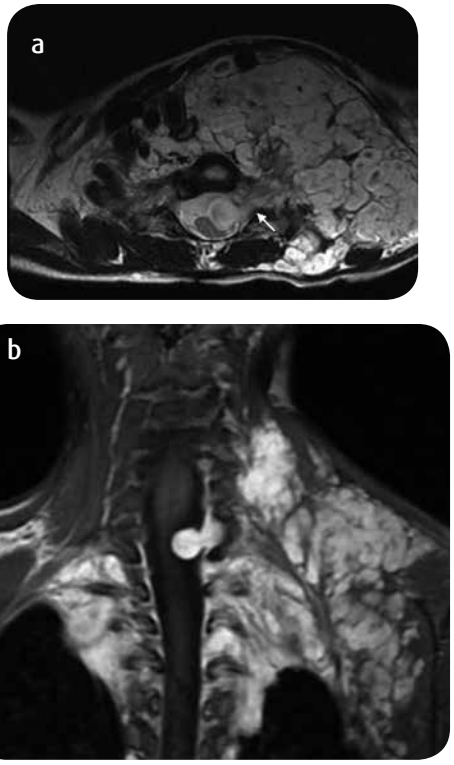

Figure 15. a) MRI, axial sequence enhanced in T2 and b) postcontrast coronal sequence enhanced in T1. The mass of high signal predominates, with central areas of low signal that originate in the cervical and thoracic nerve roots with increased size of the neural foramina (arrow) with marked compressive effect. There is extension of the lesions through the TO. These lesions correspond to neurofibromas in a patient with a known diagnosis of NF2.

Tumor lesions with ascending or descending extension

Endothoracic goiter

The growth of the thyroid gland that forms a goiter occurs in approximately 5% of the population, of which 3% to 17% extend to the thorax (40). It is usually more frequent in endemic areas of iodine deficiencies (41). It is defined as a thyroid mass that extends at least 50% below the TO (42,43). As it grows it displaces the TO structures. It is located in the anterior mediastinum (75 to 80%), below the sternum, for which reason they also receive the name of substernal goiter (40,44). When the endothoracic goiter originates from an abnormal migration of thyroid tissue it is called primary, and it is less than 1% of cases (40,45). It is characterized by having an independent vascularization, without direct connection with the thyroid gland (40). It is called secondary endothoracic goiter when the thyroid tissue extends from its normal location to the anterior mediastinum, maintaining its vascular connection (40). The endothoracic goiter maintains its connection with the gland, whether vascular, fibrous or glandular (40,46).

Endothoracic goiter originates from the anterior and inferior aspects of the thyroid lobes, proceeding anterior to the laryngeal nerve, recurrent and anterolateral to the trachea (40,45,47). In some circumstances, endothoracic goiter may extend into the posterior mediastinum (20 to 25% of cases) (40,44); it is characteristically right since the anatomical vascular barriers (innominate vein, left common carotid artery and subclavian artery) divert it to this side (40).

The CT is ideal for the identification of this entity, the density is similar to that of the thyroid tissue, in the simple slices it usually appears with high density with the density of the mass exceeding in at least 100 HU in comparison with the other soft tissues of the neck (figure 16) (40,44). Also, some calcifications can be found within the mass (40,46). The enhancement of the mass simulates the enhancement of the parenchyma of the thyroid gland (40). It is noteworthy that thyroid carcinoma is indistinguishable from a benign endothoracic goiter (32).

Fibrograse lesions: lipoma, liposarcoma, lipoblastoma

The lipomas and liposarcomas are lesions of fibrograse origin, the first of them considered a benign entity and the second one being a malignant entity. Less frequently, also, lipoblastoma (4) is included in this category, but in pediatric patients. They are frequent in the first two decades of life (4). Primary mediastinal liposarcomas are rare diagnoses that usually occur in middle-aged patients (48). Benign fibrogenous lesions are asymptomatic; however, malignant lesions may present nonspecific symptoms of chest pain, dyspnea, cough and even constitutional symptoms (48).

Lipomas are usually well-defined, encapsulated masses, which may contain fibrous septa, with fat-like behavior on CT (average density of -10 to -100 HU) and on MRI (of high signal on sequences enhanced on T1 and T2), characteristically without enhancement after the administration of contrast medium (4,49). The enhancement after administration of contrast medium or alteration in the density or intensity of the signal described with solid areas should suggest the diagnosis of liposarcoma or lipoblastoma (48,50).

Pulmonary tumors

The lung tumors that compromise the TO are those that are located in the upper lobes. Some of these tumors extend to the brachial plexus and in this case are called Pancoast tumors.

Pancoast tumors correspond to 3% of primary tumors of non-small cells (51,52). Because of their location in the pulmonary apices, the symptoms are usually not respiratory. However, they present with pain in the shoulder or Horner's syndrome (51). The extension of the anterior tumor compromises TO, especially in the tracheo-oesophageal space and, as a consequence, usually compromises the vagus nerve or the recurrent laryngeal nerve (51,53).

CT plays an important role in the determination of bone involvement, especially in the first three costal arches where the mass usually extends (figure 17). MRI allows the assessment of the extension to the soft tissues and, especially, to determine the compromise of the brachial plexus (51). Sagittal MR sequences, especially T1-weighted images, allow an adequate assessment of mass relationships with blood vessels and the brachial plexus (51,54). The obliteration of the normal fatty plane that covers the branches of the brachial plexus supposes invasion of these (51).

Tumors of the chest wall

Tumors of the chest wall are very diverse in origin, location and behavior (55). Characteristically, they are rare lesions (56). They can be benign (fibroma, neurofibroma, desmoid tumor, osteochondroma, rib fractures, among others) or malignant (neuroblastoma, rhabdomyosarcoma, Ewing's sarcoma, among others) (56). These masses, depending on their origin, can invade, expand and compress TO structures.

An example is the desmoid tumor (figure 18). It is a rare tumor, benign, but with aggressive local behavior, with a high tendency to recur after surgical excision (55). It occurs in the intercostal musculature around the shoulder, usually secondary to trauma (55). In CT, it is usually seen as a mass with soft tissue density, poorly defined, that does not enhance after administration of the contrast medium (55). In MRI, they are characteristically low signal in T1-weighted sequences and medium or high signal in T2-weighted sequences (55).

Differential diagnoses of tumors of the chest wall should include infections (especially osteomyelitis) of the rib cage or the clavicle, which can cause abscesses and pseudomasses, as well as malformations of the thoracic cavity (56).

Other tumor lesions

Any mediastinal neoplasm, especially anterior mediastinal lesions (thymoma, lymphoma, and germ cell tumors) have a greater predisposition to spread through TO.

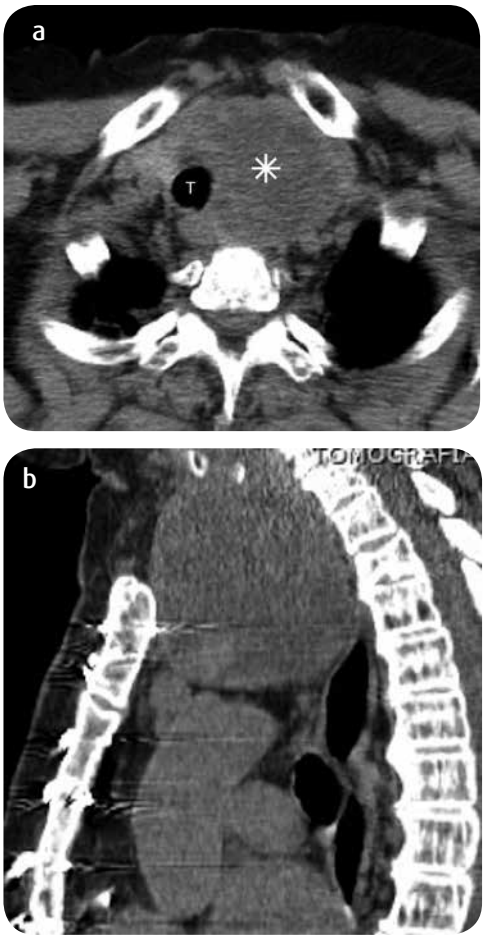

Figure 16. a) CT axial slice and b) sagittal reconstruction. Low density mass (asterisk), with some cystic areas and calcifications in the interior, which compresses and displaces the trachea to the right (T), originates in the left thyroid lobe and extends to the superior mediastinum through the TO. This finding corresponds to endothoracic goiter.

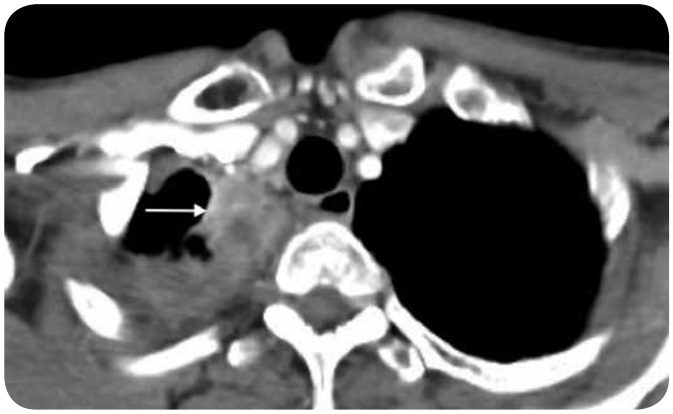

Figure 17. 63-year-old patient with lung cancer. TC axial cut. We observed mass with soft tissue density, irregular contours, with heterogeneous enhancement after the administration of the contrast medium, located in the apical segment of the right upper lobe (arrow), which loses plane of cleavage with the mediastinum at the height of the TO. There is an associated pleural effusion (not shown).

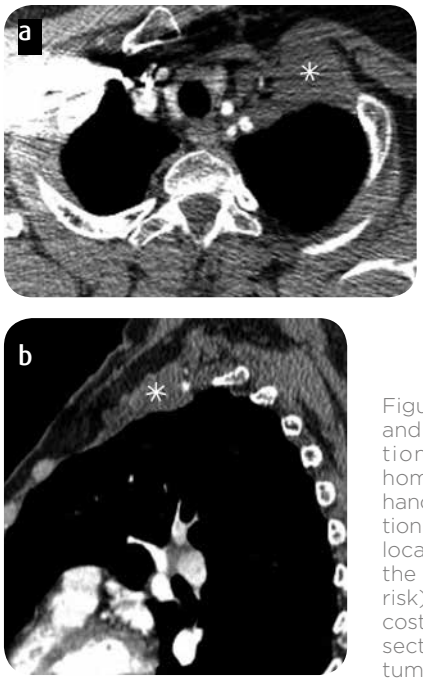

Figure 18. a) CT axial slice and b) sagittal reconstruction. Low density mass, homogeneous, without enhancement after administration of the contrast medium, located in the upper third of the left thoracic wall (asterisk) involving the first three costal arches (previously resected), related to desmoid tumor recurrence.

Germ cell tumors are gonadal, but may be of extragonadal origin, especially in the superior mediastinum, and this is the most frequent location (57). Within germ mediastinal tumors, the most frequent is the mature teratoma, the other histological subtypes are much less frequent (57). In general, the mediastinal masses are solid, homogeneous, they can have areas of cystic degeneration, calcifications or fat content, according to their histopathological origin (57).

Lymphoma in the mediastinum can be primary or be part of a disseminated disease. It can be Hodgkin or non-Hodgkin, with involvement of the mediastinum, by mass or adenomegaly, in the vast majority of cases (44,58). It occurs with equal frequency in men and women, has two age peaks of presentation, between 20 and 30 years and over 50 years (44). In CT usually found a mass located in the anterior mediastinum, homogeneous, may have areas of cystic or necrotic degeneration in up to 21 to 50% of cases (44). The mass may extend to the neck through the TO or multiple adenomegalies may be found in the TO and neck.

Conclusions

The thoracic operculum is a transition area between the neck and the thorax. Knowing the anatomy is the key to understanding and determining the lesions that pass and run through the thoracic operculum. The differential diagnosis of TO lesions is diverse and the origin of the possible lesions must be taken into account for their adequate diagnosis. Not only the sub-specialist but also the general radiologists must know their anatomy and the lesions most frequently found in this anatomical space.

Referencias

1. Chiles C, Davis KW, Williams DW III. Navigating the thoracic inlet. Radiographics. 1999;19:1161-76.
2. Parker E, Glastonbury CM. MR imaging of the thoracic inlet. Magn Reson Imaging Clin N Am. 2008;16:341-53.

3. Reede D. The thoracic inlet: normal anatomy. Semin Ultrasound CT MR. 2996;17(6):509-18.
4. Castellote A, Vázquez E, Vera J, Piqueras J, Lucaya J, García-Peña P, et al. Cervicothoracic lesions in infants and children. Radiographics. 1999;19:583-600.
5. Hanneman K, Newman B, Chan F. Congenital variants and anomalies of the aortic arch. Radiographics. 2017;37:32-51.
6. Türkvatan A, Büyükbayraktar FG, Olçer T, Cumhur T. Congenital anomalies of the aortic arch: evaluation with the use of multidetector computed tomography. Korean J Radiol. 2009;10(2):176-84.
7. Janssen M, Baggen MG, Veen HF, Smout AJ, Bekkers JA, Jonkman JG, et al. Dysphagia lusoria: clinical aspects, manometric findings, diagnosis, and therapy. Am J Gastroenterol. 2000;95(6):1411-6.
8. Tsai IC, Tzeng WS, Lee T, Jan SL, Fu YC, Chen MC, et al. Vertebral and carotid artery anomalies in patients with aberrant right subclavian arteries. Pediatr Radiol. 2007;37(10):1007-12.
9. Kim MJ, Jeong DH, Kang HH, Kim SK. A large cardiogenic thrombus lodged at the carotid bifurcation mimicking severe carotid stenosis. Neurology Asia. 2016;21(1):81-4.
10. Roy M, Roy AK, DeSanto JR, Abdelsalam M. Free floating thrombus in carotid artery in a patient with recurrent strokes. Case Reports in Medicine. 2017:2017:4932567. doi: 10.1155/2017/4932567
11. Provenzale JM. Dissection of the internal carotid and vertebral arteries: imaging features. AJR Am J Roentgenol. 1995;165:1099-104.
12. Rodallec MH, Marteau V, Gerber S, Desmottes L, Zins M. Craniocervical arterial dissection: spectrum of imaging findings and differential diagnosis. Radiographics. 2008;28:1711-28.
13. Lam WM, Ahuja AT, Mok CO, Metreweli C. Spontaneous internal jugular vein thrombosis and metastatic adenocarcinoma of unknown primary. HKMJ. 1995;1:258-60.
14. Shameem M, Akhtar J, Bhargava R, Ahmed Z, Baneen U, Khan NA. Internal jugular vein thrombosis – a rare presentation of mediastinal lymphoma. Respir Med CME. 2010;3:273-5.
15. Young CA, Menias CO, Bhalla S, Prasad SR. CT features of esophageal emergencies. Radiographics. 2008;28:1541-55.
16. Younes Z, Johnson DA. The spectrum of spontaneous and iatrogenic esophageal injury: perforations, Mallory-Weiss tears, and hematomas. J Clin Gastroenterol. 1999;29(4):306-17.
17. Cullen SN, McIntyre AS. Dissecting intramural haematoma of the oesophagus. Eur J Gastroenterol Hepatol. 2000;12(10):1151-62.
18. Lewis RB, Mehrotra AK, Rodriguez P, Levine MS. Esophageal neoplasms: radiologic-pathologic correlation. Radiographics. 2013;33:1083-108.
19. Picus D, Balfe DM, Koehler RE, Roper CL, Owen JW. Computed tomography in the staging of esophageal carcinoma. Radiology. 1983;146(2):433-8.
20. Pinto A, Scaglione M, Scuderi MG, Tortora G, Daniele S, Romano L. Infections of the leading to descending necrotizing mediastinitis: Role of multi-detector row computed tomography. Eur J Radiol. 2008;65:389-94.
21. Prince JS, Duhamel DR, Levin DL, Harrell JH, Friedman PJ. Nonneoplastic lesions of the tracheobronchial Wall: radiologic findings with bronchoscopic correlation. Radiographics. 2002;22:S215-30.
22. Kim YH, Kim HT, Lee KS, Uh ST, Cung YT, Park CS. Serial fiberoptic bronchoscopic observations of endobronchial tuberculosis before and early after antituberculosis chemotherapy. Chest. 1993;103:673-7.
23. Soto-Hurtado EJ, Peñuela-Ruiz L, Rivera-Sánchez I, Torres-Jiménez J. Tracheal diverticulum: a review of the literature. Lung. 2006;184:303-7.
24. Frenkiel S, Assimes IK, Rosales JK. Congenital tracheal diverticulum. A case report. Ann Otol Rhinol Laryngol. 1980;89:406-8.
25. Sayit AT, Elmali M, Saglam D, Celenk C. The diseases of airway-tracheal diverticulum: a review of the literatura. J Thoracic Dis. 2016;8(10):E1163-7.
26. Bhatnagar V, Lal R, Agarwal S, Mitra DK. Endoscopic treatment of tracheal diverticulum after primary repair of esophageal atresia and tracheoesophageal fistula. J Pediatr Surg. 1998;33:1323-4.
27. Rahalkar MD, Lakhkar DL, Joshi SW, Gundawar S. Tracheal diverticula. Report of 2 cases. Ind J Radiol Imag. 2004;14:197-8.
28. Lazzarini de Oliveira LC, Costa de Barros Franco CA, Gomes de Salles CL, de Oliveira AC. A 38 year old man with tracheomegaly, tracheal diverticulosis, and bronchiectasias. Chest. 2001;120:1018-20.
29. Early E, Bothwell M. Congenital tracheal diverticulum. Otolaryngol Head Neck Surg. 2002;127:119-21.
30. Han S, Dikmen E, Aydin S, Yapakci O. Tracheal diverticulum: a rare cause of dysphagia. Eur J Cardiothorac Surg. 2008;34(4):916-7.
31. Raman SP, Pipavath SNJ, Raghu G, Schmidt RA, Godwin JD. Imaging of thoracic lymphatic diseases. AJR Am J Roentgenol. 2009;193:1504-13.
32. Glazer HS, Siegel MJ, Sagel SS. Low-Attenuation mediastinal masses on CT. AJR Am J Roentgenol. 1989;152:1173-7.
33. Shaffer K, Rosado-de-Christenson ML, Patz Jr. EF, Farver CF. Thoracic lymphangioma in adults: CT and MR imaging features. AJR Am J Roentgenol. 1994;162:283-9.
34. Seeger M, Bewig B, Günther R, Schafmayer C, Vollnberg B, Rubin D, et al. Terminal part of the thoracic duct: high-resolution US imaging. Radiology. 2009;252(3):897-904.
35. Liu ME, Branstetter BF, Whetstone J, Escott EJ. Normal CT appearance of the distal thoracic duct. AJR Am J Roentgenol. 2006;187:1615-20.
36. Gossner J. Appearance and visibility of the thoracic duct on computed tomography of the chest. Internet J Radiol. 2009;12(2):1-5.
37. Mikityansky I, Zager EL, Yousem DM, Loevner LA. MR imaging of the brachial plexus. Magn Reson Imaging Clin N Am. 2012;20(4):791-826.
38. Yoshikawa T, Hayashi N, Yamamoto S, Tajiri Y, Yoshioka N, Masumoto T, et al. Brachial plexus injury: clinical manifestations, conventional imaging findings, and the latest imaging techniques. Radiographics. 2006;26:S133-43.
39. Shaham D, Skilakaki MG, Goitein O. Imaging of the mediastinum: applications for thoracic surgery. Thorac Surg Clin. 2004;14(1):25-42.
40. Buckley JA, Stark P. Intrathoracic mediastinal thyroid goiter: imaging manifestations. AJR Am J Roentgenol. 1999;173:471-5.
41. Aguiar-Quevedo K, Cerón-Navarro J, Jordá-Aragón C, Pastor-Martínez E, Sales-Badia JG, García-Zarza A, et al. Intrathoracic goiter: a literature review. Cir Esp. 2010;88(3):142-5.
42. Al Hashemi A, Gallo R, Shah MT, Al Fairi A, Al Amir A, Al Shraim M, et al. Giant intrathoracic goiter. Int J Surg Open. 2016(2):6-10.
43. Katlic MR, Wang CA, Grillo HC. Subesternal goiter. Ann Thorac Surg. 1985;39(4):391-9.
44. Tecce PM, Fishman EK, Kuhlman JE. CT evaluation of the anterior mediastinum: Spectrum of disease. Radiographics. 1994;14:973-90.
45. Madjar S. Weissberg D. Retrosternal goiter. Chest. 1995:108:78-82.
46. Glazer HS, Molina PL, Siegel MJ, Sagel SS. High-attenuation mediastinal masses on unenhanced CT. AJR Am J Roentgenol. 1991;156:45-50.
47. Mack E. Management of patients with substemal goiters. Surg Clin North Am. 1995:75(3):377-94.
48. Munden RF, Nesbitt JC, Kemp BL, Chasen MH, Whitman GJ. Primary liposarcoma of the mediastinum. AJR Am J Roentgenol. 2000;175:1340.
49. Occhipinti M, Heidinger BH, Franquet E, Eisenberg RL, Bankier AA. Imaging the posterior mediastinum: a multimodality approach. Diagn Interv Radiol. 2015;21(4):293-306.
50. Eisenstat R, Bruce D, Williams LE, Katz DS. Primary liposarcoma of the mediastinum with coextistent mediastinal lipomatosis. AJR Am J Roentgenol. 2000;174:572-3.
51. Bruzzi JF, Komaki R, Walsh GL, Truong MT, Gladish GW, Munden RF, et al. Imaging of non-small cell lung cancer of the superior sulcus. Radiographics. 2008;28:551-60.
52. Ginsberg RJ, Martini N, Zaman M, et al. Influence of surgical resection and brachytherapy in the management of superior sulcus tumor. Ann Thorac Surg. 1994;57(6):1440-5.
53. Arcasoy SM, Jett JR. Superior pulmonary sulcus tumors and Pancoast's syndrome. N Engl J Med. 1997;337(19):1370-6.
54. Heelan RT, Demas BE, Caravelli JF, Martini N, Bains MS, McCormack PM, et al. Superior sulcus tumors: CT and MR imaging. Radiology. 1989;170:637-41.
55. Jeung MY, Gangi A, Gasser B, Vasilescu C, Massard G, Wihlm JM, et al. Imaging of chest wall disorders. Radiographics. 1999;19:617-37.
56. Watt AJB. Chest wall lesions. Paediatr Respir Rev. 2000 (3):328-38.
57. Rosado-de-Christenson ML, Templeton PA, Moran CA. Mediastinal germ cell tumors: radiologic and pathologic correlation. Radiographics. 1992;12:1013-30.
58. Fishman EK, Kuhlman JE, Jones RJ. CT of lymphoma: spectrum of disease. Radiographics. 1991;11:647-69.

Correspondencia

Felipe Aluja Jaramillo
Country Scan Ltda.
Carrera 16 # 84A-09, consult. 323
Bogotá, Colombia
macario171@gmail.com

Recibido para evaluación: 28 de julio de 2017
Aceptado para publicación: 17 de octubre de 2017